Indian Journal of Pure & Applied Physics
Vol. 52, November 2014, pp. 725-737

Series solution of unsteady Eyring Powell nanofluid flow on a rotating cone

S Nadeem & S Saleem[1]*
[1]Department of Mathematics, Quaid-i-Azam University 45320, Islamabad 44000, Pakistan
*E-mail: salmansaleem_33@hotmail.com

Received 25 November 2013; revised 18 April 2014; accepted 10 September 2014

In the present paper, unsteady mixed convective flow on a rotating cone in a rotating nano Eyring Powell nanofluid has been studied. It has been revealed that a self-similar solution is only possible when the free stream angular velocity and the angular velocity of the cone are inversely proportional to a linear function of time. The boundary layer equations are reduced to the nonlinear ordinary differential equations using similarity and non-similarity transformations. The reduced coupled nonlinear differential equations for rotating cone are solved by optimal homotopy analysis method. The physical behaviour of pertinent parameters has also been studied through the graphs of dimensionless velocities, temperature, nano particle volume fraction, skin friction, Nusselt number and Sherwood number. Numerical results for important physical quantities are reported.

Keywords: Mixed convection, Heat transfer, Nano Eyring Powell nanofluid, Buongiorno model, OHAM solutions

1 Introduction

Flow of non-Newtonian fluids has attained a great success in the theory of fluid mechanics due to its applications in biological sciences and industry. A few applications of non-Newtonian fluids are food mixing and chyme movement in the intestine, polymer solutions, paint, flow of blood, flow of nuclear fuel slurries, flow of liquid metals and alloys, flow of mercury amalgams and lubrications with heavy oils and greases[1-6]. The concept of rotating flows over a rotating body is extensively used in design of turbines and turbo machines in meteorology, gaseous and nuclear reactors, stabilized missiles. An impressive application in this regard is the cooling of nose-cone of re-entry vehicle by spinning nose[7].

Free convection is due to the difference of temperature at different locations of fluid and forced convection is a flow of heat caused due to some external force. By combining both of them, the phenomena of mixed convection take place. This nature of convection occurs in many practical applications like electronic devices cooled by fans, heat exchanger placed at low velocity environment, solar central receive to wind current etc. In the present study, a vertical cone is rotating about its vertical axis of symmetry in a rotating non-Newtonian nanofluid. This rotation of cone produces a circumferential velocity in the fluid through the involvement of viscosity. When the temperature of cone and the free stream fluid differs, there will be a transfer of energy as well as density of the fluid also changes. In a gravitational field, this results in an additional force, namely buoyancy force besides due to the act of centrifugal force field. In most of the situations moderate flow velocities and large wall fluid temperature differences, both the buoyancy as well as the centrifugal force are in a compatible order and the convective heat transfer process is named as mixed convection[8]. The effects of Prandtl number on the heat transfer on rotating non-isothermal disks and cones have been studied by Harnett and Deland[9]. Hering and Grosh[10] have investigated the steady mixed convection from a vertical cone for small Prandtl number. They applied similarity transformation which show Buoyancy parameter is the dominant dimensionless parameter that would set the three regions, specifically forced, free and mixed convection. Himasekhar *et al*[11]. have investigated the similarity solution of the mixed convection flow over a vertical rotating cone in a fluid for a wide range of Prandtl numbers. Hasen and Majumdar[12] have presented the steady double diffusive mixed convection flow along a vertical cone under the combined buoyancy effect of thermal species diffusion. Non-similar solutions to the heat transfer in unsteady mixed convection flows from a vertical cone were obtained by Kumari and Pop[13]. Boundary layers on a rotating cones, discs and axisymmetric surfaces with a concentrated heat sources have been studied by

Wang[14]. All the above mentioned works refer to steady flows. However, in many situations the flows and the angular velocity both are useful if unsteady flow are taken into account. Ece[15] has developed the solution for small time for unsteady boundary layer flow of an impulsively started translating a spinning rotational symmetric body. Anil Kumar and Roy[16] presented the self-similar solutions of an unsteady mixed convection flow over a rotating cone in a rotating fluid. They found that similar solutions are only possible when angular velocity is inversely proportional to time. The effect of combined viscous dissipation and Joule heating on unsteady mixed convention magnetohydrodynamics (MHD) flow on a rotating cone in an electrically conducting rotating fluid in the presence of Hall and ion-slip currents has been investigated by Osalusi *et al*[17]. Moreover, the analytical treatment of unsteady mixed convection MHD flow on a rotating cone in a rotating frame has been studied by Nadeem and Saleem[18].

In last few decades, study about the convective transport of nanofluids has attained much attention by the researchers due to its property to enhance the thermal conductivity as compared to base fluid. The word nanofluid is referred to the fluids in which suspension of nano-scale particles and the base fluid is being incorporated. This concept was proposed by Choi[20]. He revealed that by adding of a slight amount of nano particles to conventional heat transfer liquids improved the thermal conductivity of the fluid approximately two times. Another recent application of nanofluid flow is nano-drug delivery[21]. Suspension of metal nanoparticle is also being developed for other purpose, such as medical applications including cancer therapy. Also the nanofluids are frequently used as coolants, lubricants and micro-channel heat sinks. Nanofluids mostly consist of metals, oxides or carbon nanotubes. Buongiorno[22] introduced seven slip mechanisms between nano particles and the base fluid. He showed that the Brownian motion and thermophoresis have effected significantly in the laminar forced convection of nanofluids. Based on this finding, he developed non-homogeneous two-component equations in nanofluids. Nield and Kuznetsov[23] presented an analytical treatment of double-diffusive natural convection boundary layer flow in a porous medium saturated by nanofluid. Some experimental and theoretical works related to nanofluids are given in Refs (24-27).

In general, it is problematic to handle nonlinear problems, specifically in an analytical way. Perturbation techniques like variation of iteration method (VIM) and homotopy perturbation method[27] (HPM) were mostly used to get solutions of such mathematical analysis. These techniques are dependent on the small/large constraints, the supposed perturbation quantity. Unluckily, various nonlinear physical situations in real life do not always have such type of perturbation parameters. Further, both of the perturbation procedures themselves cannot give a modest approach in order to regulate or control the region and rate of convergence series. Liao[28] offered an influential analytic technique to solve the nonlinear problems, explicitly the homotopy analysis method[28-34] (HAM). It offers a suitable approach to control and adjust the convergence region and rate of approximation series, once required.

The objective of the present study is to examine the unsteady mixed convection flow on a rotating cone in a rotating nano Eyring Powell fluid. The governing parabolic partial differential equations are reduced to nonlinear coupled ordinary differential equations by applying the similarity transformations. The solution of reduced equations is obtained by using optimal homotopy analysis method. It is found that similarity solutions are only possible when angular velocity is inversely proportional to time.

2 Physical Model

The time dependent axisymmetric, incompressible flow on an infinite rotating cone in a rotating nano Eyring-Powell fluid has been considered. The time dependent rotations of the cone as well as fluid about the axis of cone either in the assisting or opposing direction is responsible for the unsteadiness in the flow. The physical model for the given problem is shown in Fig. 1. Rectangular curvilinear fixed coordinate system is used for the flow problem. Let u, v and w be the velocity components along (tangential), (circumferential or azimuthal) and (normal) directions, respectively. The effects of buoyancy forces arise due to both temperature and concentration variations in the fluid flow. Further, it is assumed that the wall and the free stream are kept at a constant temperature and concentration. Also the effects of viscous dissipation are ignored.

The extra stress tensor in an Eyring-Powell fluid model is given by:

$$\bar{\mathbf{S}} = \mu ? \bar{\mathbf{V}} + \frac{1}{\beta} \mathrm{Si}nh^{-1}(\frac{1}{c} ? \bar{\mathbf{V}})$$

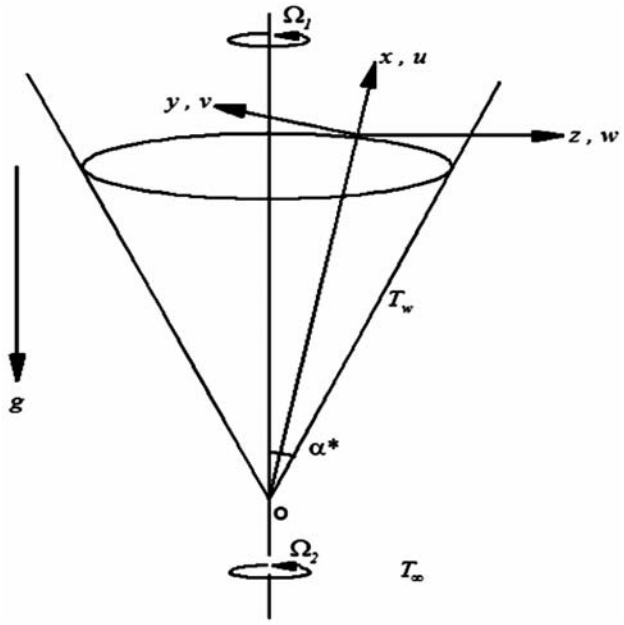

Fig. 1 — Sketch of the problem

where $\bar{\mathbf{V}}$ is the velocity, $\bar{\mathbf{S}}$ is the Cauchy stress tensor, μ is the shear viscosity, β and c are the material constants. Considering:

$$\sin h^{-1}\left(\frac{1}{c}?\bar{\mathbf{V}}\right)\approx\frac{1}{c}?\bar{\mathbf{V}}-\frac{1}{6}\left(\frac{1}{c}?\bar{\mathbf{V}}\right)^3,\left|\frac{1}{c}?\bar{\mathbf{V}}\right|-1$$

After the boundary layer analysis and using the Boussinesq approximations, the governing equations for motion, temperature and nano particle volume fraction for non-Newtonian nanofluid are stated as :

$$\frac{\partial(xu)}{\partial x}+\frac{\partial(xw)}{\partial z}=0 \qquad \ldots(1)$$

$$\frac{\partial u}{\partial t}+u\frac{\partial u}{\partial x}+w\frac{\partial u}{\partial z}-\frac{v^2}{x}=-\frac{v_e^2}{x}+g\xi\cos\alpha^*\left(T-T_\infty\right)$$
$$+g\xi^*\cos\alpha^*\left(C-C_\infty\right)+\left(\nu+\frac{1}{\rho\beta c}\right)\frac{\partial^2 u}{\partial z^2}$$
$$-\frac{1}{6\rho\beta c^3}\left[\left(\frac{\partial u}{\partial z}\right)^2\left\{\frac{4}{x}\frac{\partial u}{\partial x}+\frac{2}{x}\frac{\partial w}{\partial z}+4\frac{\partial^2 u}{\partial x^2}+2\frac{\partial^2 w}{\partial x\partial z}\right\}\right.$$
$$-\frac{\partial u}{\partial z}\frac{\partial v}{\partial z}\left\{\frac{3}{x}\frac{\partial v}{\partial x}+\frac{2v}{x^2}-2\frac{\partial^2 v}{\partial x^2}\right\}$$
$$+\frac{\partial u}{\partial z}\frac{\partial^2 u}{\partial z\partial x}\left\{16\frac{\partial u}{\partial x}+8\frac{\partial w}{\partial z}\right\}$$
$$-\left(\frac{\partial v}{\partial z}\right)^2\left\{\frac{2}{x}\frac{\partial w}{\partial z}+\frac{6u}{x^2}+\frac{2}{x}\frac{\partial u}{\partial x}+\frac{\partial^2 w}{\partial z\partial x}\right\}$$
$$+\frac{\partial v}{\partial x}\frac{\partial v}{\partial z}\left\{2\frac{\partial^2 w}{\partial z^2}+4\frac{\partial^2 u}{\partial z\partial x}\right\}\frac{\partial^2 u}{\partial z^2}\left\{4\left(\frac{\partial u}{\partial x}\right)^2\right.$$
$$\left.+4\frac{\partial u}{\partial x}\frac{\partial w}{\partial z}+\frac{v^2}{x^2}+\left(\frac{\partial v}{\partial x}\right)^2-\frac{2v}{x}\frac{\partial v}{\partial x}+4\left(\frac{\partial w}{\partial z}\right)^2\right\}$$
$$+\frac{\partial v}{\partial x}\frac{\partial^2 v}{\partial z^2}\left\{2\frac{\partial u}{\partial x}+\frac{2u}{x}+2\frac{\partial w}{\partial z}\right\}+\frac{\partial^2 v}{\partial x\partial z}\left\{\frac{2u}{x}\frac{\partial v}{\partial z}\right.$$
$$\left.+2\frac{\partial v}{\partial z}\frac{\partial w}{\partial z}-\frac{4v}{x}\frac{\partial u}{\partial z}+4\frac{\partial u}{\partial z}\frac{\partial v}{\partial x}+2\frac{\partial u}{\partial x}\frac{\partial v}{\partial z}\right\}$$
$$+\frac{\partial^2 v}{\partial z^2}\left\{-\frac{2uv}{x^2}+2\frac{\partial v}{\partial z}\frac{\partial w}{\partial x}-\frac{2v}{x}\frac{\partial w}{\partial z}-\frac{2v}{x}\frac{\partial u}{\partial x}\right\}$$
$$\left.-\frac{4v}{x}\frac{\partial^2 u}{\partial x\partial z}\frac{\partial v}{\partial z}+\frac{\partial^2 w}{\partial z^2}\left\{-\frac{2v}{x}\frac{\partial v}{\partial z}+8\frac{\partial u}{\partial z}\frac{\partial w}{\partial z}+\frac{\partial u}{\partial x}\frac{\partial u}{\partial z}\right\}\right] \qquad \ldots(2)$$

$$\frac{\partial v}{\partial t}+u\frac{\partial v}{\partial x}+w\frac{\partial v}{\partial z}+\frac{uv}{x}=\frac{\partial v_e}{\partial t}+\left(\nu+\frac{1}{\rho\beta c}\right)\frac{\partial^2 v}{\partial z^2}$$
$$-\frac{1}{6\rho\beta c^3}\left[\left(\frac{\partial u}{\partial z}\right)^2\left\{\frac{\partial^2 v}{\partial x^2}-\frac{3v}{x^2}\right\}+\frac{\partial^2 u}{\partial z\partial x}\left\{4\frac{\partial u}{\partial z}\frac{\partial v}{\partial x}\right.\right.$$
$$\left.-\frac{4v}{x}\frac{\partial u}{\partial z}+\frac{2u}{x}\frac{\partial v}{\partial z}+2\frac{\partial u}{\partial x}\frac{\partial v}{\partial z}+2\frac{\partial v}{\partial z}\frac{\partial w}{\partial z}\right\}$$
$$+\frac{\partial^2 v}{\partial x\partial z}\left\{\frac{4u}{x}\frac{\partial u}{\partial z}+2\frac{\partial u}{\partial x}\frac{\partial u}{\partial z}-\frac{2v}{x}\frac{\partial v}{\partial z}\right\}$$
$$+\frac{\partial u}{\partial z}\frac{\partial v}{\partial z}\left\{\frac{2}{x}\frac{\partial u}{\partial x}+\frac{8u}{x^2}\right\}+\frac{\partial^2 u}{\partial z^2}\left\{2\frac{\partial u}{\partial x}\frac{\partial v}{\partial x}+2\frac{\partial v}{\partial z}\frac{\partial w}{\partial x}\right.$$
$$+2\frac{\partial v}{\partial x}\frac{\partial w}{\partial z}-\frac{2v}{x}\frac{\partial u}{\partial x}-\frac{2v}{x}\frac{\partial w}{\partial z}+\frac{2u}{x}\frac{\partial v}{\partial x}-\frac{2uv}{x^2}\Big\}$$
$$+\frac{\partial^2 v}{\partial z^2}\{2\frac{\partial u}{\partial z}\frac{\partial w}{\partial x}+\left(\frac{\partial v}{\partial x}\right)^2+\frac{v^2}{x^2}-\frac{2v}{x}\frac{\partial v}{\partial x}+\frac{4u^2}{x^2}$$
$$+\frac{4u}{x}\frac{\partial w}{\partial z}+4\left(\frac{\partial w}{\partial z}\right)^2\Big\}+\frac{\partial^2 w}{\partial z^2}\left\{-\frac{2v}{x}\frac{\partial u}{\partial z}+\frac{4u}{x}\frac{\partial v}{\partial z}\right.$$
$$\left.+8\frac{\partial v}{\partial z}\frac{\partial w}{\partial z}\right\}-\frac{\partial^2 v}{\partial z^2}\frac{\partial w}{\partial z}-\frac{\partial v}{\partial x}\frac{\partial^2 w}{\partial z^2}-\frac{2}{x}\frac{\partial u}{\partial z}\frac{\partial v}{\partial z}$$
$$\left.-\frac{\partial^2 u}{\partial x\partial z}\frac{\partial v}{\partial z}-\frac{\partial u}{\partial z}\frac{\partial^2 v}{\partial x\partial z}\right] \qquad \ldots(3)$$

$$\frac{\partial T}{\partial t}+u\frac{\partial T}{\partial x}+w\frac{\partial T}{\partial z}=\alpha\frac{\partial^2 T}{\partial z^2}+\tau\left[D_B\frac{\partial C}{\partial z}\frac{\partial T}{\partial z}+\frac{D_T}{T_\infty}\left(\frac{\partial T}{\partial z}\right)^2\right] \quad \ldots(4)$$

$$\frac{\partial C}{\partial t}+u\frac{\partial C}{\partial x}+w\frac{\partial C}{\partial z}=D_B\frac{\partial^2 C}{\partial z^2}+\frac{D_T}{T_\infty}\frac{\partial^2 T}{\partial z^2} \quad \ldots(5)$$

Making use of the following similarity transformations[16] in Eqs (1-5):

$$v_e=\Omega_2 x\sin\alpha^*(1-st^*)^{-1}$$
$$\eta=\left(\frac{\Omega\sin\alpha^*}{v}\right)^{1/2}(1-st^*)^{-1/2}z$$
$$t^*=(\Omega\sin\alpha^*)t$$
$$u(t,x,z)=-2^{-1}\Omega x\sin\alpha^*(1-st^*)^{-1}f'(\eta)$$
$$v(t,x,z)=\Omega x\sin\alpha^*(1-st^*)^{-1}g(\eta)$$
$$w(t,x,z)=(v\Omega\sin\alpha^*)^{1/2}(1-st^*)^{-1/2}f(\eta)$$
$$T(t,x,z)=T_\infty+(T_w-T_\infty)\theta(\eta)$$
$$T_w-T_\infty=(T_0-T_\infty)\left(\frac{x}{L}\right)(1-st^*)^{-2}$$
$$C(t,x,z)=C_\infty+(C_w-C_\infty)\varphi(\eta)$$
$$(C_w-C_\infty)=(C_0-C_\infty)\left(\frac{x}{L}\right)(1-st^*)^{-2}$$
$$Gr_1=g\xi\cos\alpha^*(T_0-T_\infty)\frac{L^3}{v^2},\ \mathrm{Re}_L=\Omega\sin\alpha^*\frac{L^2}{v}$$
$$\mathrm{Pr}=\frac{v}{\alpha},\ \lambda_1=\frac{Gr_1}{\mathrm{Re}_L^2},\ Gr_2=g\xi\cos\alpha^*(C_0-C_\infty)\frac{L^3}{v^2}$$
$$\lambda_2=\frac{Gr_2}{\mathrm{Re}_L^2},\ \gamma=\frac{\Omega_1}{\Omega},\ N=\frac{\lambda_2}{\lambda_1},\ \delta=\frac{1}{\mu\beta c}$$
$$\kappa=\frac{1}{6\mu\beta c^3}(\Omega\sin\alpha^*)^2(1-st^*)^{-2} \quad \ldots(6)$$

where T is the temperature, C the nano particle volume fraction, g the gravity, α the thermal diffusivity, α^* the semi-vertical angle of the cone, υ the kinematic viscosity, ρ the density, ξ and ξ^* are the volumetric coefficient of expansion for temperature and concentration, respectively, C_∞ and T_∞ are the free stream concentration and temperature, respectively, δ and κ are the flow parameters for Eyring Powell model. Also τ is the ratio of nano particle heat capacity and the base fluid heat capacity, D_B is the Brownian diffusion coefficient and D_T is the thermophoresis diffusion coefficient. By using the above mentioned similar and non-similar variables of Eq. (6), Eq. (1) is identically satisfied and Eqs (2-5) give:

$$(1+\delta)f'''-ff''+2^{-1}f'^2-2[g^2-(1-\gamma)^2]-2\lambda_1(\theta+N\varphi)-s(f'+2^{-1}\eta f'')+\kappa[8f'(f'')^2-f''gg'+4f'(g')^2-3(f')^2f'''+2f'''g^2]=0 \quad \ldots(7)$$

$$(1+\delta)g''-(fg'-gf')+s(1-\gamma-g-2^{-1}\eta g')+\kappa\left(\frac{1}{4}(f'')^2g+12f'f''g'+3(f')^2g''-2g(g')^2\right)=0 \quad \ldots(8)$$

$$\theta''-\mathrm{Pr}\left[\left(f\theta'-f'\frac{\theta}{2}\right)-s\left(2\theta+2^{-1}\eta\theta'\right)+Nb\varphi'\theta'+Nt(\theta')^2\right]=0 \quad \ldots(9)$$

$$\varphi''-Le\left[\left(f\varphi'-f'\frac{\varphi}{2}\right)-s(2\varphi+2^{-1}\eta\varphi')\right]\mathrm{Pr}+\frac{Nt}{Nb}\theta''=0 \quad \ldots(10)$$

$$f(0)=0=f'(0),\ g(0)=\gamma,\ \theta(0)=\varphi(0)=1$$
$$f'(\infty)=0,\ g(\infty)=1-\gamma,\ \theta(\infty)=\varphi(\infty)=0 \quad \ldots(11)$$

$$Nb=\frac{(\rho c)_p D_B(C_B-C_\infty)}{\upsilon(\rho c)_f},\ Nt=\frac{(\rho c)_p D_T(T_w-T_\infty)}{\upsilon(\rho c)_f T_\infty}$$
$$Le=\frac{v}{D_B}$$

in which Nb is the Brownian motion parameter, Nt is the thermophoresis parameter and Le is the Lewis number, λ_1 is the buoyancy force parameter and the ratio of the Grash of numbers is denoted by N, which measures the relative importance of thermal diffusion in inducing the buoyancy forces which drive the flow. It has zero contribution for chemical diffusion, tends to infinity for the thermal diffusion and possesses a positive value when the buoyancy forces due to temperature and concentration difference act in the same direction and vice versa. s is the unsteady parameter and the flow is assisting for positive values

of s and vice versa. Moreover $\gamma = 0$ shows that only the fluid is rotating but the cone is at rest. The fluid and the cone are rotating with equal angular velocity in the same direction for $\gamma = 0.5$ and for $\gamma = 1$, only the cone is rotating while keeping the fluid at rest. The coefficient of local surface skin friction in $x-$ and $y-$ directions, the local Nusselt number and local Sherwood number in dimensionless forms are given by:

$$C_{fx}\,\mathrm{Re}_x^{\frac{1}{2}} = [-(1+\delta)f'' - \kappa\{(f')^2 f'' - 4f'gg'\}]_{\eta=0}$$
$$C_{fy}\,\mathrm{Re}_x^{\frac{1}{2}} = -[2(1+\delta)g' - \kappa\{f'f''g + (\dot{f})^2 g'\}]_{\eta=0} \quad \ldots(12)$$

$$Nu\,\mathrm{Re}_x^{-\frac{1}{2}} = -\theta'(0),\ Sh\,\mathrm{Re}_x^{-\frac{1}{2}} = -\varphi'(0) \quad \ldots(13)$$

where $\mathrm{Re}_x = \dfrac{\Omega x^2 \sin\alpha^*(1-st^*)^{-1}}{\nu}$ is the Reynolds number, $Nu = -\dfrac{\left[k\left(\frac{\partial T}{\partial z}\right)\right]_{z=0}}{T_w - T\infty}$ is the Nusselt number and $Sh = -\dfrac{\left[\rho D\left(\dfrac{\partial C}{\partial z}\right)\right]_{z=0}}{C_w - C_\infty}$ is the Sherwood number. Note that when $\kappa = \delta = Nb = Nt = 0$ in Eqs (7-8) our problem reduces to the problem of viscous flow[16]. Since the aim of the authors is to find the self-similar solutions, so Eqs (7-10) are solved with boundary conditions given in Ref. (11). Self-similar solution means that the solution at different times may be reduced to a single solution i.e., the solution at one value of time t is the same to the solution at any other value of time t. This similarity property reduces the number of independent variables to one.

3 Methodology of the Problem

We choose the following base functions for the HAM solutions:

$$\{\eta^k \exp(-n\eta) \,|\, k \geq 0, n \geq 0\} \quad \ldots(14)$$

$$f(\eta) = a_{0,0}^0 + \sum_{n=0}^{\infty}\sum_{k=0}^{\infty} a_{m,n}^k \eta^k \exp(-n\eta) \quad \ldots(15)$$

$$g(\eta) = b_{0,0}^0 + \sum_{n=0}^{\infty}\sum_{k=0}^{\infty} b_{m,n}^k \eta^k \exp(-n\eta) \quad \ldots(16)$$

$$\theta(\eta) = \sum_{n=0}^{\infty}\sum_{k=0}^{\infty} c_{m,n}^k \eta^k \exp(-n\eta) \quad \ldots(17)$$

$$\varphi(\eta) = \sum_{n=0}^{\infty}\sum_{k=0}^{\infty} d_{m,n}^k \eta^k \exp(-n\eta) \quad \ldots(18)$$

in which $a_{m,n}^k,\ b_{m,n}^k,\ c_{m,n}^k,\ d_{m,n}^k$ are the coefficients. These provide us with solution expressions of $f(\eta),\ g(\eta),\ \theta(\eta)$ and $\varphi(\eta)$, respectively. The initial approximations are $f_0,\ g_0,\ \theta_0$ and φ_0 with the respective auxiliary linear operators are:

$$f_0(\eta) = 0 \quad \ldots(19)$$

$$g_0(\eta) = (1-\gamma) + (2\gamma - 1)\exp(-\eta) \quad \ldots(20)$$

$$\theta_0(\eta) = \exp(-\eta) \quad \ldots(21)$$

$$\varphi_0(\eta) = \exp(-\eta) \quad \ldots(22)$$

And the auxiliary linear operators are:

$$\pounds_f = \frac{d^3 f}{d\eta^3} - \frac{df}{d\eta} \quad \ldots(23)$$

$$\pounds_g = \frac{d^2 g}{d\eta^2} + \frac{dg}{d\eta} \quad \ldots(24)$$

$$\pounds_\theta = \frac{d^2\theta}{d\eta^2} - \theta \quad \ldots(25)$$

$$\pounds_\varphi = \frac{d^2\varphi}{d\eta^2} - \varphi \quad \ldots(26)$$

The operators given in Eqs $(23-26)$ have the following properties

$$\pounds_f[C_1 + C_2\exp(\eta) + C_3\exp(-\eta)] = 0 \quad \ldots(27)$$

$$\pounds_g[C_4 + C_5\exp(-\eta)] = 0 \quad \ldots(28)$$

$$\pounds_\theta[C_6\exp(\eta) + C_7\exp(-\eta)] = 0 \quad \ldots(29)$$

$$\pounds_{\varphi}[C_8\exp(\eta)+C_9\exp(-\eta)]=0 \qquad \ldots(30)$$

where $C_i\,(i=1-9)$ are arbitrary constants. Let $p\in[0,1]$ be an embedding parameter $\hbar_f$, $\hbar_g$, $\hbar_\theta$ and $\hbar_\varphi$ are the non zero auxiliary parameters. The problems at the zeroth order are given:

$$(1-p)\pounds_f[\hat{f}(\eta;p)-\hat{f}_0(\eta)]=p\hbar_f N_f[\hat{f}(\eta;p),\ \hat{g}(\eta;p),\hat{\theta}(\eta;p),\hat{\varphi}(\eta;p)] \qquad \ldots(31)$$

$$(1-p)\pounds_g[\hat{g}(\eta;p)-\hat{g}_0(\eta)]=p\hbar_g N_g[\hat{f}(\eta;p),\ \hat{g}(\eta;p)] \qquad \ldots(32)$$

$$(1-p)\pounds_\theta[\hat{\theta}(\eta;p)-\hat{\theta}_0(\eta)]=p\hbar_\theta N_\theta[\hat{f}(\eta;p),\ \hat{\theta}(\eta;p),\hat{\varphi}(\eta;p)] \qquad \ldots(33)$$

$$(1-p)\pounds_\varphi[\hat{\varphi}(\eta;p)-\hat{\varphi}_0(\eta)]=p\hbar_\varphi N_\varphi[\hat{f}(\eta;p),\ \hat{\theta}(\eta;p),\hat{\varphi}(\eta;p)] \qquad \ldots(34)$$

$$\hat{f}(0;p)=0=\hat{f}'(0;p)\ ,\ \hat{g}(0;p)=\gamma_1,\quad \hat{\theta}(0;p)=\hat{\varphi}(0;p)=1 \qquad \ldots(35)$$

$$\hat{f}'(\infty;p)=0\ ,\hat{f}''(\infty;p)=0,\ \hat{g}(\infty;p)=1-\gamma_1,\quad \hat{g}'(\infty;p)=0,\ \hat{\theta}(\infty;p)=\hat{\varphi}(\infty;p)=0, \qquad \ldots(36)$$

and the nonlinear operators

$$\begin{aligned}N_f[\hat{f}(\eta;p),\hat{g}(\eta;p),\hat{\theta}(\eta;p),\hat{\varphi}(\eta;p)]&=(1+\delta)\frac{\partial^3\hat{f}(\eta;p)}{\partial\eta^3}\\&-\hat{f}(\eta;p)\frac{\partial^2\hat{f}(\eta;p)}{\partial\eta^2}+\frac{1}{2}\left(\frac{\partial\hat{f}(\eta;p)}{\partial\eta}\right)^2\\&+\kappa\left(8\frac{\partial\hat{f}(\eta;p)}{\partial\eta}\left(\frac{\partial^2\hat{f}(\eta;p)}{\partial\eta^2}\right)^2-\frac{\partial^2\hat{f}(\eta;p)}{\partial\eta^2}\hat{g}(\eta;p)\frac{\partial\hat{g}(\eta;p)}{\partial\eta}\right)\\&-3\kappa\left(\left(\frac{\partial\hat{f}(\eta;p)}{\partial\eta}\right)^2\frac{\partial^3\hat{f}(\eta;p)}{\partial\eta^3}+2\frac{\partial^3\hat{f}(\eta;p)}{\partial\eta^3}\hat{g}(\eta;p)^2\right)\\&-2\lambda_1(\hat{\theta}(\eta;p)+N\hat{\varphi}(\eta;p))\\&-s\left(\frac{\partial\hat{f}(\eta;p)}{\partial\eta}+\frac{1}{2}\eta\frac{\partial^2\hat{f}(\eta;p)}{\partial\eta^2}\right)\\&-2[(\hat{g}(\eta;p))^2-(1-\alpha_1)^2]\\&+4\kappa\frac{\partial\hat{f}(\eta;p)}{\partial\eta}\left(\frac{\partial\hat{g}(\eta;p)}{\partial\eta}\right)^2\end{aligned} \qquad \ldots(37)$$

$$\begin{aligned}N_g[\hat{g}(\eta;p),\hat{f}(\eta;p)]&=(1+\delta)\frac{\partial^2\hat{g}(\eta;p)}{\partial\eta^2}\\&-\left[\hat{f}(\eta;p)\frac{\partial\hat{g}(\eta;p)}{\partial\eta}-\hat{g}(\eta;p)\frac{\partial\hat{f}(\eta;p)}{\partial\eta}\right]\\&+s\left(1-\alpha_1-\hat{g}(\eta;p)-\frac{1}{2}\eta\frac{\partial\hat{g}(\eta;p)}{\partial\eta}\right)\\&+\kappa\left[\frac{1}{4}\left(\frac{\partial^2\hat{f}(\eta;p)}{\partial\eta^2}\right)^2\hat{g}(\eta;p)\right.\\&+12\frac{\partial\hat{f}(\eta;p)}{\partial\eta}\frac{\partial^2\hat{f}(\eta;p)}{\partial\eta^2}\frac{\partial\hat{g}(\eta;p)}{\partial\eta}\\&+3\left(\frac{\partial^2\hat{f}(\eta;p)}{\partial\eta^2}\right)^2\frac{\partial^2\hat{g}(\eta;p)}{\partial\eta^2}\\&\left.-2\hat{g}(\eta;p)\left(\frac{\partial\hat{g}(\eta;p)}{\partial\eta}\right)^2\right]\end{aligned} \qquad \ldots(38)$$

$$\begin{aligned}N_\theta[\hat{\theta}(\eta;p),\hat{f}(\eta;p)]&=\frac{1}{\Pr}\frac{\partial^2\hat{\theta}(\eta;p)}{\partial\eta^2}\\&-\left(\hat{f}(\eta;p)\frac{\partial\hat{\theta}(\eta;p)}{\partial\eta}-\frac{1}{2}\frac{\partial\hat{f}(\eta;p)}{\partial\eta}\hat{\theta}(\eta;p)\right)\\&-s\left(2\hat{\theta}(\eta;p)+\frac{1}{2}\eta\frac{\partial\hat{\theta}(\eta;p)}{\partial\eta}\right)\\&+Nb\frac{\partial\hat{\varphi}(\eta;p)}{\partial\eta}\frac{\partial\hat{\theta}(\eta;p)}{\partial\eta}+Nt\left(\frac{\partial\hat{\theta}(\eta;p)}{\partial\eta}\right)^2\end{aligned} \qquad \ldots(39)$$

$$\begin{aligned}N_\varphi[\hat{\varphi}(\eta;p),\hat{f}(\eta;p)]&=\frac{\partial^2\hat{\varphi}(\eta;p)}{\partial\eta^2}\\&-\Pr Le\left(\hat{f}(\eta;p)\frac{\partial\hat{\varphi}(\eta;p)}{\partial\eta}-\frac{1}{2}\frac{\partial\hat{f}(\eta;p)}{\partial\eta}\hat{\varphi}(\eta;p)\right)\\&-s\left(2\hat{\varphi}(\eta;p)+\frac{1}{2}\eta\frac{\partial\hat{\varphi}(\eta;p)}{\partial\eta}\right)Le\Pr+\frac{Nt}{Nb}\frac{\partial^2\hat{\theta}(\eta;p)}{\partial\eta^2}\end{aligned} \qquad \ldots(40)$$

For $p=0$ and $p=1$, we have:

$$\hat{f}(\eta;0)=f_0(\eta),\ \hat{f}(\eta;1)=f(\eta) \quad \ldots(41)$$

$$\hat{g}(\eta;0)=g_0(\eta),\ \hat{g}(\eta;1)=g(\eta) \quad \ldots(42)$$

$$\hat{\theta}(\eta;0)=\theta_0(\eta),\ \hat{\theta}(\eta;1)=\theta(\eta) \quad \ldots(43)$$

$$\hat{\varphi}(\eta;0)=\varphi_0(\eta),\ \hat{\varphi}(\eta;1)=\varphi(\eta). \quad \ldots(44)$$

when p varies from 0 to 1, then the initial guesses vary from $f_0(\eta)$, $g_0(\eta)$, $\frac{-b\pm\sqrt{b^2-4ac}}{2a}$ $\theta_0(\eta)$, $\frac{n!}{r!(n-r)!}$ $\varphi_0(\eta)\frac{1}{2}$ to $f(\eta)$, $g(\eta)$, $\theta(\eta)$, $\varphi(\eta)$, respectively. Due to Taylor's series with respect to p, we have:

$$\hat{f}(\eta;p)=f_0(\eta)+\sum_{m=1}^{\infty}f_m(\eta)\,p^m \quad \ldots(45)$$

$$\hat{g}(\eta;p)=g_0(\eta)+\sum_{m=1}^{\infty}g_m(\eta)\,p^m \quad \ldots(46)$$

$$\hat{\theta}(\eta;p)=\theta_0(\eta)+\sum_{m=1}^{\infty}\theta_m(\eta)\,p^m \quad \ldots(47)$$

$$\hat{\varphi}(\eta;p)=\varphi_0(\eta)+\sum_{m=1}^{\infty}\varphi_m(\eta)\,p^m \quad \ldots(48)$$

$$\begin{aligned} f_m(\eta)&=\frac{1}{m!}\frac{\partial^m f(\eta;p)}{\partial\eta^m}\bigg|_{p=0}\\ g_m(\eta)&=\frac{1}{m!}\frac{\partial^m g(\eta;p)}{\partial\eta^m}\bigg|_{p=0} \quad \ldots(49)\\ \theta_m(\eta)&=\frac{1}{m!}\frac{\partial^m \theta(\eta;p)}{\partial\eta^m}\bigg|_{p=0}\\ \varphi_m(\eta)&=\frac{1}{m!}\frac{\partial^m \varphi(\eta;p)}{\partial\eta^m}\bigg|_{p=0} \quad \ldots(50)\end{aligned}$$

and

$$f(\eta)=f_0(\eta)+\sum_{m=1}^{\infty}f_m(\eta) \quad \ldots(51)$$

$$g(\eta)=g_0(\eta)+\sum_{m=1}^{\infty}g_m(\eta) \quad \ldots(52)$$

$$\theta(\eta)=\theta_0(\eta)+\sum_{m=1}^{\infty}\theta_m(\eta) \quad \ldots(53)$$

$$\varphi(\eta)=\varphi_0(\eta)+\sum_{m=1}^{\infty}\varphi_m(\eta) \quad \ldots(54)$$

The mth-order deformation problems are defined as:

$$\pounds_f[f_m(\eta)-\chi_m f_{m-1}(\eta)]=\hbar_f R_m^f(\eta) \quad \ldots(55)$$

$$\pounds_g[g_m(\eta)-\chi_m g_{m-1}(\eta)]=\hbar_g R_m^g(\eta) \quad \ldots(56)$$

$$\pounds_\theta[\theta_m(\eta)-\chi_m \theta_{m-1}(\eta)]=\hbar_\theta R_m^\theta(\eta) \quad \ldots(57)$$

$$\pounds_\varphi[\varphi_m(\eta)-\chi_m \varphi_{m-1}(\eta)]=\hbar_\varphi R_m^\varphi(\eta) \quad \ldots(58)$$

$$f_m(0)=f_m'(0)=g_m(0)=\theta_m(0)=\varphi_m(0)=0 \quad \ldots(59)$$

$$\begin{aligned} f_m'(\infty)&=g_m(\infty)=f_m''(\infty)=g_m'(\infty)=\theta_m(\infty)\\ &=\varphi_m(\infty)=0 \end{aligned} \quad \ldots(60)$$

$$\begin{aligned} R_m^f(\eta)&=(1+\delta)f_{m-1}'''-2\lambda_1(\theta_{m-1}+N\varphi_{m-1})\\ &\quad -s\left(f_{m-1}'+\frac{1}{2}\eta f_{m-1}'''\right)-\sum_{k=0}^{m-1}\left(f_k f_{m-1-k}''+\frac{1}{2}f_k'\ f_{m-1-k}'\right)\\ &\quad -2\left[\sum_{k=0}^{m-1}g_k g_{m-1-k}-(1-\gamma)^2\right]\\ &\quad +\kappa\sum_{k=0}^{m-1}\begin{pmatrix}8f_{m-1-k}''\sum_{l=0}^{k}f_{k-l}''f_l'-f_{m-1-k}''\sum_{l=0}^{k}g_{k-l}g_l'\\ +4f_{m-1-k}'\sum_{l=0}^{k}g_{k-l}'g_l'-3f_{m-1-k}'''\sum_{l=0}^{k}f_{k-l}'f_l'\\ +2f_{m-1-k}'''\sum_{l=0}^{k}g_{k-l}g_l\end{pmatrix} \end{aligned} \quad \ldots(61)$$

$$\begin{aligned} R_m^g(\eta)&=(1+\delta)g_{m-1}''-\sum_{k=0}^{m-1}[f_k g_{m-1-k}'-g_k f_{m-1-k}']\\ &\quad +s\left(1-\gamma-g_{m-1}-\frac{1}{2}\eta g_{m-1}'\right)\\ &\quad +\kappa\sum_{k=0}^{m-1}\begin{pmatrix}\frac{1}{4}g_{m-1-k}\sum_{l=0}^{k}f_{k-l}''f_l''+12f_{m-1-k}'\sum_{l=0}^{k}f_{k-l}''g_l'\\ +3g_{m-1-k}''\sum_{l=0}^{k}f_{k-l}'f_l'-2g_{m-1-k}\sum_{l=0}^{k}g_{k-l}'g_l'\end{pmatrix} \end{aligned} \quad \ldots(62)$$

$$R_m^{\theta}(\eta)=\frac{1}{\Pr}\theta''_{m-1}-\sum_{k=0}^{m-1}\left[f_k\theta'_{m-1-k}-\frac{1}{2}\theta_k f'_{m-1-k}\right]$$
$$-s\left(2\theta_{m-1}+\frac{1}{2}\eta\theta'_{m-1}\right)+Nb\sum_{k=0}^{m-1}\varphi'_k\theta'_{m-1}+Nt\sum_{k=0}^{m-1}\theta'_k\theta'_{m-1} \quad \ldots(63)$$

$$R_m^{\varphi}(\eta)=\varphi''_{m-1}-Le\Pr\left\{\sum_{k=0}^{m-1}\left[f_k\varphi'_{m-1-k}-\frac{1}{2}\varphi_k f'_{m-1-k}\right]\right.$$
$$\left.-s\left(2\varphi_{m-1}+\frac{1}{2}\eta\varphi'_{m-1}\right)\right\}+\frac{Nt}{Nb}\theta''_{m-1} \quad \ldots(64)$$

$$\chi_m=\begin{cases}0 & m\le 1\\ 1 & m>1\end{cases} \quad \ldots(65)$$

The general solutions of Eqs (55-58) are:

$$f_m(\eta)=f_m^*(\eta)+C_1+C_2\exp(\eta)+C_3\exp(-\eta) \quad \ldots(66)$$

$$g_m(\eta)=g_m^*(\eta)+C_4+C_5\exp(-\eta) \quad \ldots(67)$$

$$\theta_m(\eta)=\theta_m^*(\eta)+C_6\exp(\eta)+C_7\exp(-\eta) \quad \ldots(68)$$

$$\varphi_m(\eta)=\varphi_m^*(\eta)+C_8\exp(\eta)+C_9\exp(-\eta) \quad \ldots(69)$$

in which $f_m^*(\eta), g_m^*(\eta), \theta_m^*(\eta)$ and $\varphi_m^*(\eta)$ denote the special solutions of Eqs (55-58) and the integral constants $C_i (i=1-9)$ are determined by employing the boundary conditions given in Eqs (59) and (60). It is noted that to satisfy the boundary conditions at infinity, we must set $C_2=C_6=C_8=0$. Note that Eqs. $(55)-(58)$ can be solved by Mathematica one after the other in the order $m=1,2,3....$

4 Optimal Convergence-control Parameters

It is seen that the series solutions obtained by HAM, contain the non-zero auxiliary parameters c_0^f, c_0^g, c_0^{θ} and c_0^{φ}, which determine the convergence-region and rate of the homotopy series solutions. In order to determine the optimal values of c_0^f, c_0^g, c_0^{θ} and c_0^{φ} it is used here the average residual error[29] defined by:

$$\varepsilon_m^f=\frac{1}{k+1}\sum_{j=0}^{k}\left[N_f\left(\sum_{i=0}^{m}\hat{f}(\eta),\sum_{i=0}^{m}\hat{g}(\eta),\sum_{i=0}^{m}\hat{\theta}(\eta),\sum_{i=0}^{m}\hat{\varphi}(\eta)\right)_{y=j\delta y}\right]^2 dy \quad \ldots(70)$$

$$\varepsilon_m^g=\frac{1}{k+1}\sum_{j=0}^{k}\left[N_g\left(\sum_{i=0}^{m}\hat{f}(\eta),\sum_{i=0}^{m}\hat{g}(\eta)\right)_{y=j\delta y}\right]^2 dy \quad \ldots(71)$$

$$\varepsilon_m^{\theta}=\frac{1}{k+1}\sum_{j=0}^{k}\left[N_{\theta}\left(\sum_{i=0}^{m}\hat{f}(\eta),\sum_{i=0}^{m}\hat{\theta}(\eta),\sum_{i=0}^{m}\hat{\varphi}(\eta)\right)_{y=j\delta y}\right]^2 dy \quad \ldots(72)$$

$$\varepsilon_m^{\varphi}=\frac{1}{k+1}\sum_{j=0}^{k}\left[N_{\varphi}\left(\sum_{i=0}^{m}\hat{f}(\eta),\sum_{i=0}^{m}\hat{\theta}(\eta),\sum_{i=0}^{m}\hat{\varphi}(\eta)\right)_{y=j\delta y}\right]^2 dy \quad \ldots(73)$$

Following Liao[29] :

$$\varepsilon_m^t=\varepsilon_m^f+\varepsilon_m^g+\varepsilon_m^{\theta}+\varepsilon_m^{\varphi} \quad \ldots(74)$$

where ε_m^t is the total squared residual error, $\delta y=0.5,\ k=20.$ Total average squared residual error is minimized by using symbolic computation software Mathematica. We have directly applied the command Minimize to obtain the corresponding local optimal convergence control parameters. Tables 1 and 2 are presented for the case of single optimal convergence control parameter. It is found that the averaged squared residual errors and total averaged squared residual errors are getting smaller and smaller as we increase the order of approximation. Therefore, Optimal Homotopy Analysis Method gives us relaxation to select any set of local convergence control parameters to obtain convergent results.

5 Results and Discussion

The effects of ratio of angular velocities of the cone and the fluid γ, flow parameters κ and δ on the velocity, temperature and nano particle volume

Table 1 — Total averaged squared residual errors using single optimal convergence control parameter c_0

m	c_0	$\varepsilon^t{}_m$
2	$^{-}$0.99	8.77×10^{-3}
4	$^{-}$0.87	4.34×10^{-3}
6	$^{-}$0.75	4.11×10^{-3}

Table 2 — Average squared residual errors using Table

m	2	4	6
$\varepsilon^f{}_m$	8.22×10^{-5}	8.20×10^{-5}	8.17×10^{-5}
$\varepsilon^g{}_m$	2.71×10^{-3}	1.36×10^{-3}	1.26×10^{-3}
$\varepsilon^{\theta}{}_m$	3.58×10^{-4}	2.71×10^{-4}	2.67×10^{-4}
$\varepsilon^{\theta}{}_m$	5.62×10^{-3}	2.63×10^{-3}	2.49×10^{-3}

fraction which are presented in graphical and tabular form, have been studied. These effects have been analyzed in Figs (2-6). The behaviour of both velocities (i.e. tangential and azimuthal) for combined effects of γ and λ_1 are displayed in Fig. 2(a and b), respectively. The direction of both the fluid and the cone is same while rotating with an equal angular velocity for $\gamma = 0.5$. The positive Buoyancy force i.e. $\lambda_1 = 1$ which behaves as favourable pressure gradient is a source for the flow. For $\gamma > 0.5$, the tangential velocity $-f'(\eta)$ has an increasing magnitude, while the azimuthal velocity $g(\eta)$ shows reduction in its behaviour. Further for $\gamma < 0.5$ the variation is opposite. The asymptotic behaviour at the edge of boundary layer of both velocities is observed for negative values of γ and $\lambda_1 = 1$. Physically, these oscillations are caused by surplus convection of angular momentum appears in the boundary layer region. Figure 3(a and b) shows the behaviour of tangential velocity $-f'(\eta)$ and azimuthal velocity $g(\eta)$ for different values of κ, respectively. It is shown that the tangential velocity $-f'(\eta)$ decreases as the values of κ goes higher. On the other hand, the azimuthal velocity $g(\eta)$ shows an increasing attitude.

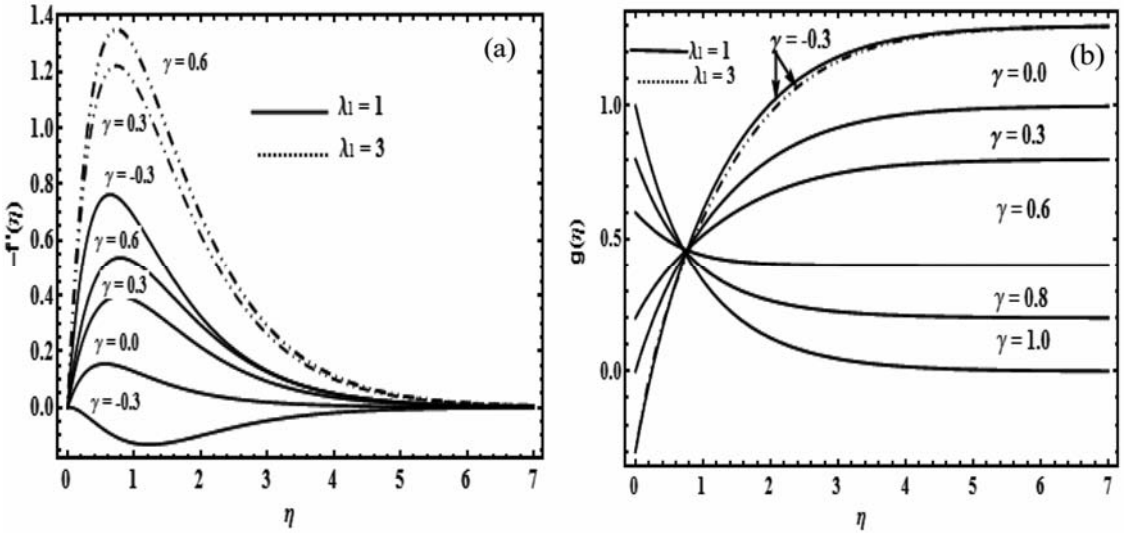

Fig. 2 — (a) and (b) Effects of γ on velocities $-f''(\eta)$ and $g(\eta)$

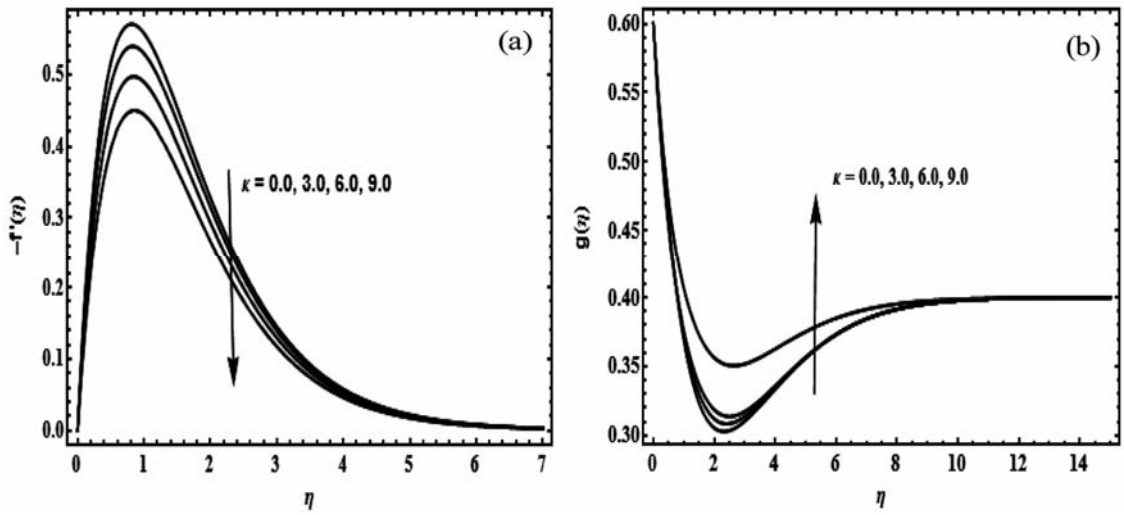

Fig. 3 — (a) and (b) Effects of κ on velocities $-f''(\eta)$ and $g(\eta)$

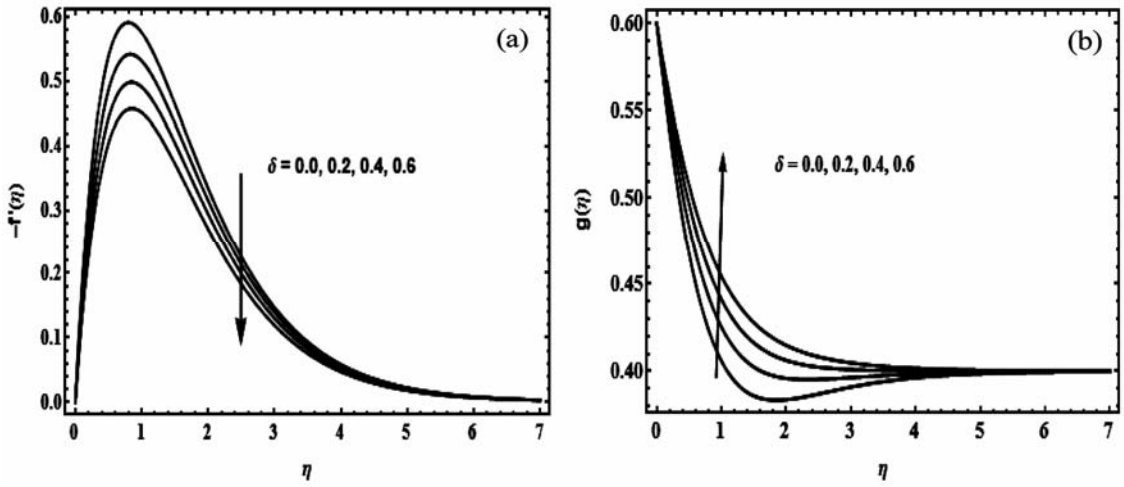

Fig. 4 — (a) and (b) Effects of δ on velocities $-f''(\eta)$ and $g(\eta)$

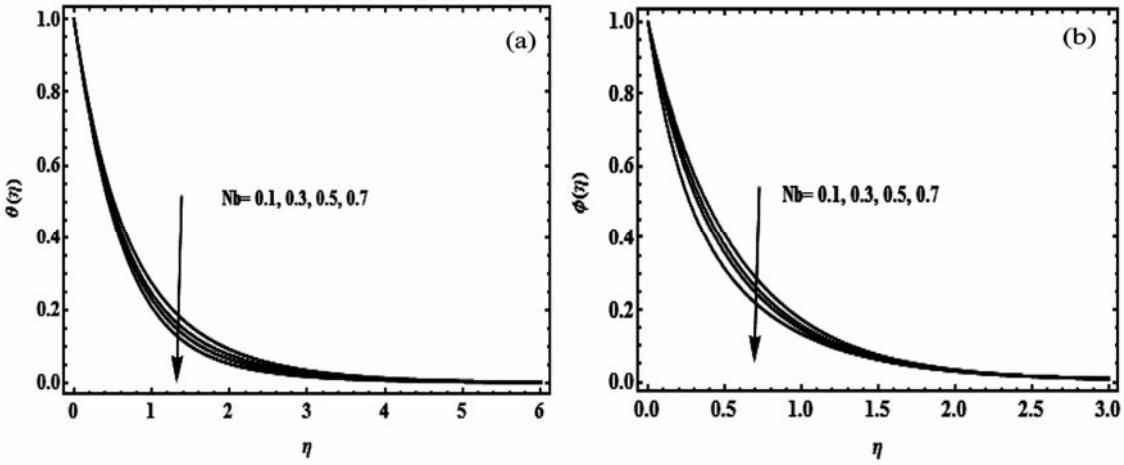

Fig. 5 — (a) and (b) Effect of *Nb* of temperature $\theta(\eta)$ and nano particle volume fraction $\varphi(\eta)$

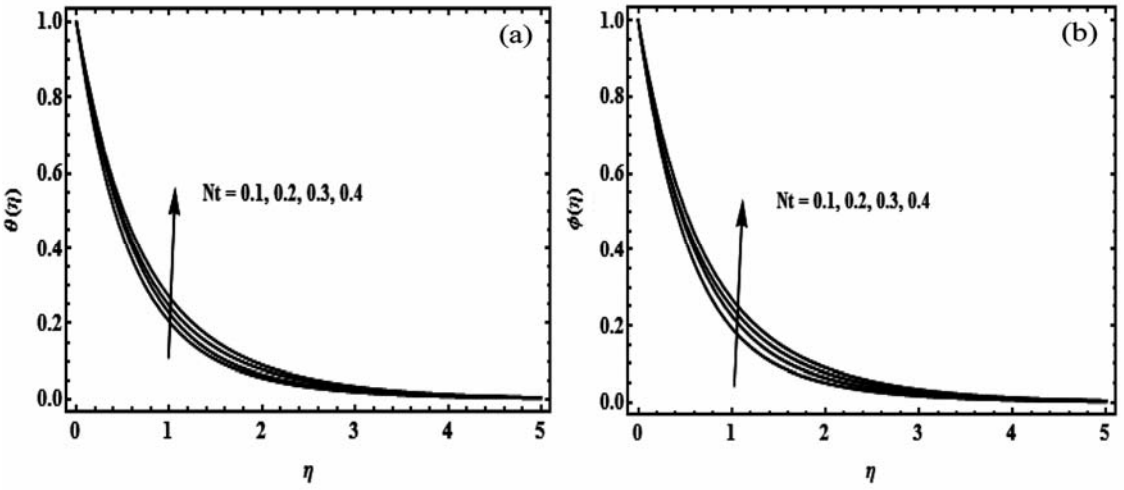

Fig. 6 — (a) and (b) Effect of *Nt* of temperature $\theta(\eta)$ and nano particle volume fraction $\varphi(\eta)$

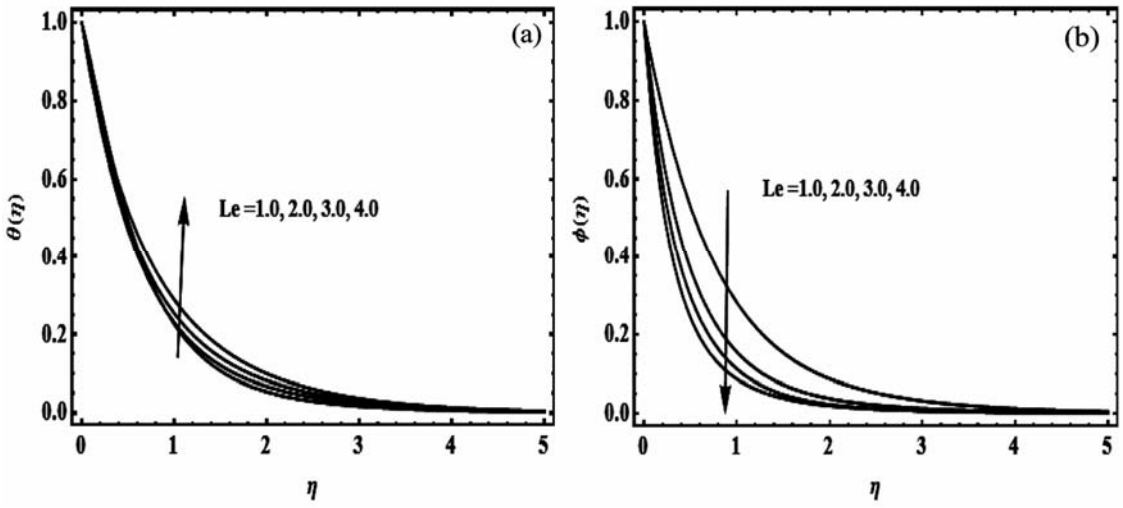

Fig. 7 — (a) and (b) Effect of *Le* on temperature $\theta(\eta)$ and nano particle volume fraction $\varphi(\eta)$

In Fig. 4(a and b), the effect of flow parameter δ has been displayed for tangential velocity $-f'(\eta)$ and azimuthal velocity $g(\eta)$, respectively. It is obvious from Fig. (4) that the variation of both velocities is same when compared with Fig. 3(a and b). Figure 5(a and b) shows the effect of Brownian motion parameter Nb on temperature field $\theta(\eta)$ and nano particle volume fraction $\varphi(\eta)$. Figure 5 shows that the temperature profile $\theta(\eta)$ increases and nano particle volume fraction $\varphi(\eta)$ decreases with increasing values of Nb. It is perceived from Fig. 6(a and b), that the temperature field $\theta(\eta)$ and nano particle volume fraction $\varphi(\eta)$ increase by increasing thermophoresis parameter Nt. Figure 7(a and b) shows the effects of Lewis number Le on temperature profile $\theta(\eta)$ and nano particle volume fraction $\varphi(\eta)$. It is seen that the variation of thermal and concentration boundary layer thickness is opposite. The effects of Prandtl number Pr on temperature profile is shown in Fig. 8. The thermal boundary layer decreases with an increase in Prandtlnumber Pr. This is due to the fact that higher Prandtl number Pr fluid has a lower thermal conductivity which causes in thinner thermal boundary layer and therefore, the heat transfer rate rises. For engineering problems, the heat transfer rate should be small. This can be maintained by keeping the low temperature difference between the surface and the free stream fluid, using a low Prandtl number fluid, keeping the surface at a constant temperature instead of at a constant heat flux, and by applying the

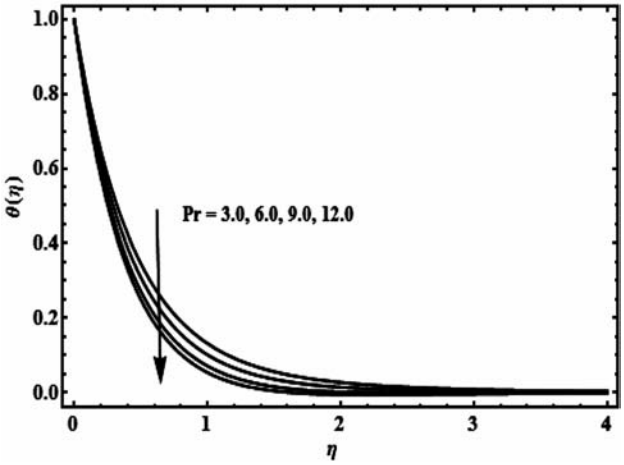

Fig. 8 — Effect of *Pr* on temperature $\theta(\eta)$

buoyancy force in the opposite direction to that of forced flow. A decent agreement of our present OHAM results with the previous literature[16] is shown in Table 3. The numerical values of Skin friction coefficients in both the directions for flow parameters κ, δ and N are given in Table 4. Table 4 indicates that skin friction coefficient in tangential direction decreases for κ but all the other physical quantities show an increasing variation for increasing values of κ, δ and N. Table 5 is given for the tabular values of local Nusselt number and local Sherwood number for various nano parameters and the Prandtl number Pr. It is seen that local Nusselt number is an increasing function of Prandtl number Pr whereas for all nano parameters (i.e Nb, Nt and Le) it shows a decreasing variation. Moreover the variation of local Sherwood

Table 3 — Comparison of OHAM results and numerical results when $\kappa=\delta=Nb=Nt=0$

		Present Analytical results			Numerical results (16)		
λ	γ	$C_{fx}\mathrm{Re}_x^{1/2}$	$C_{fy}\mathrm{Re}_x^{1/2}$	$Nu\mathrm{Re}_x^{1/2}$	$C_{fx}\mathrm{Re}_x^{1/2}$	$C_{fy}\mathrm{Re}_x^{1/2}$	$Nu\mathrm{Re}_x^{1/2}$
1	0	0.63246	−0.63944	0.81920	0.63241	−0.63949	0.81922
	0.25	1.31335	−0.22768	0.89013	1.31339	−0.22765	0.89011
	0.50	1.84792	0.19801	0.93702	1.84798	0.19806	0.93700
	0.75	2.24659	0.62678	0.96559	2.24659	0.62679	0.96563

Table 4 — Numerical values of skin friction coefficients, Nusselt and Sherwood number for different values of flow parameters

κ	δ	N	$C_{fx}\mathrm{Re}_x^{1/2}$	$C_{fy}\mathrm{Re}_x^{1/2}$
0.0	0.1	1.5	1.66944	0.58071
2.0			1.58909	0.96232
4.0			1.499329	0.792263
6.0			1.42216	0.882214
0.5	0.0		1.60897	0.348824
	0.2		1.69295	0.371421
	0.4		1.76433	0.390617
	0.6		1.82896	0.40728
		0.5	1.07557	0.328872
		1.0	1.36409	0.344709
		1.5	1.65298	0.360525
		2.0	1.94261	0.376439

Table 5 — Numerical values of local Nusselt and local Sherwood number for different values of ano particles and prandtl number

Nb	Nt	Le	Pr	$-\varphi(0)$	$-\varphi(0)$
0.1				1.52283	4.36434
0.2				1.46255	4.40248
0.3				1.40385	4.44033
0.4				1.34672	4.4779
	0.2			1.4913	2.17068
	0.3			1.46113	2.18952
	0.4			1.43226	2.20779
	0.5			1.40462	2.2255
		1.0		1.55862	1.25304
		2.0		1.54135	2.15127
		3.0		1.53588	2.98137
		4.0		1.52436	4.36434
			2.0	1.78767	4.03333
			4.0	2.37234	3.91851
			6.0	2.68937	3.87781
			8.0	2.87964	3.85701

number is just opposite to the local Nusselt number for the concerning pertinent parameters.

6 Conclusions

In the present paper, the unsteady mixed convection flow of rotating Eyring-Powell nanofluid on a rotating cone is examined. The reduced non-dimensional differential equations are solved by optimal homotopy analysis method. The present results are found to be in acceptable agreement with the prior available results in literature. The concluding results are as follows:

The tangential velocity $-f'(\eta)$ decreases for increasing values of flow parameters κ and δ, but the behaviour is just opposite for azimuthal velocity $g(\eta)$. The temperature field increases as all the nano parameters increase.The nano particle volume fraction $\varphi(\eta)$ is a decreasing function of Brownian motion parameter N_b and Lewis number Le. The increase in Prandtl number Pr reduces the thermal boundary layer.The skin friction coefficients increase its magnitude due to an increase in ratio of buoyancy forces N and flow parameter δ, but shows a reverse attitude for κ.

References

1 Patel M &Timol M G, *Int J Appl Math Mech*, 6 (2010) 79.
2 Nadeem S & Akbar N K, *J Taiwan InstChem Eng*, 42 (2011) 58.
3 Ellahi R, *Commun Nonlinear SciNumer Simul*, 14 (2009) 1377.
4 Nadeem S, Haq R U & Lee C, *Sci Iran*, 19 (2012) 1550.
5 Powell R E &Eyring H, *Nature*, 154 (1944) 427.
6 Akbar N S &Nadeem S, *Int J Heat Mass Trans*, 55 (2012) 375.
7 Ostrach S & Brown W H, *NACA T N* , (1958) 4323.
8 Anilkumar D & Roy S, *Int J Heat Mass Trans*, 47 (2004) 1673.
9 Hartnett J P & Deland E C, J Heat Trans, 83 (1961) 95.
10 Hering R G &GroshR J, *ASME J Heat Trans*, 85 (1963) 29.
11 Himasekhar K, Sarma P K &Anardhan K, *Int Commun Heat Mass Trans*, 16 (1989) 99.

12 Hasan H &MajundarA S, *Int J Energy Res*, 9 (1985) 129.
13 Kumari M, Pop I &Nath G, *Int Commun Heat Mass Trans*, 16 (1989) 247.
14 Wang C Y, *Acta Mech*, 81 (1990) 245.
15 Ece M C, *J Eng Math*, 26 (1992) 415.
16 Anilkumar D & Roy S, *Appl Math Comput*, 155 (2004) 545.
17 Osalusi E, Side J, Harris R & Clark P, *Inter Commun Heat Mass Trans,* 35(4) (2008) 413.
18 Nadeem S & Saleem S, *J Taiwan Inst Chem Engg*, 44(4) (2013) 596.
19 Ahmed N, Goswami J K &Barua D P, *Indian J Pure Appl Math*, 44(4) (2013)443.
20 Choi S U S, *Developments & Applications of Non-Newtonian Flows*, 66 (1995) 99.
21 Kleinstreuer C, Li J & Koo J, *Int J Heat Mass Trans*, 51 (2008) 5590.
22 Buongiorno J, *ASME J Heat Trans*, 128 (2006) 240.
23 Nield D A & Kuznetsov A V,*Int J Heat Mass Trans*, 54 (2011) 374.
24 Nadeem S &Saleem S, *J Thermophy Heat Trans*, 28(2) (2014) 295.
25 Khan Z H, Khan WA & Pop I, *Int J Heat Mass Trans*, 66 (2013) 603.
26 Ellahi R, *Appl Math Model*, 37(3) (2013) 1451.
27 Zafar H Khan, Rahim Gul& Waqar A Khan, *Proceedings of the Asme Summer Heat Transfer Conference*, 1 (2009) 301.
28 Liao S J, *Beyond perturbation: Introduction to the homotopy analysis method*, Chapman & Hall/CRC Press, Boca Raton, 2003.
29 Liao S J, *Comm Nonlinear Sci Numer Simulat*, 15 (2010) 2003.
30 FazleMabood, Waqar A Khan & Ahmad IzaniMd Ismail, *Inter J Modern Engg Sci*, 2(2) (2013) 63.
31 Ellahi R, Raza M &Vafai K, *Math Comput Model*, 55 (2012) 1876.
32 Abbasbandy S, *Phys Lett*, 60 (2006) 109.
33 Ellahi R &Riaz A, *Math Comp Model*, 52 (2010) 1783.
34 Nadeem S & Saleem S, *Appl Nano Sci*, 4 (2014) 405.